The Role Played by Orbital Energetics in Solvent Mediated Electronic Coupling†

R. Kaplan,‡ A. M. Napper,§ D. H. Waldeck,*,§ and M. B. Zimmt*,‡

Chemistry Department, Brown University, Providence, Rhode Island 02912, and Chemistry Department, University of Pittsburgh, Pittsburgh, Pennsylvania 15260

Received: April 26, 2001; In Final Form: September 26, 2001

Electron-transfer rates are measured for three supramolecular species, which contain an electron donor, electron acceptor, and rigid connecting bridge. Two of the species are linear and the third species is C-shaped. The latter topology produces a 10 Å wide, solvent accessible gap between the donor and the acceptor units. This molecular design allows the dependence of the electron-transfer rate on the solvent's electronic character to be evaluated. The results display a strong correlation between the energy of the solvent's lowest unoccupied molecular orbital and the magnitude of solvent mediated electronic coupling in systems with electronically excited donors. The variation of the electronic coupling with solvent modulates transfer rate constants by more than an order of magnitude.

Introduction

For many long distance electron transfer systems, the factors controlling transfer dynamics are sufficiently understood to permit reasonable interpretation of rate constants. Within semiclassical formulations, nonadiabatic electron-transfer rate constants are expressed as the product of a Franck Condon weighted density of states (*fcwds*), which determines the probability that the system attains the transition state geometry, and an electron tunneling probability, which characterizes the primary electronic event (see eq 1).[1] The *fcwds* and activation barriers may be estimated with models that account for molecular shape, changes in charge distributions, and the relevant properties of the medium (solvent). The tunneling probability is determined by the electronic coupling |V| between the electron donor (D) and acceptor (A) groups in the transition state geometry and depends on the molecular and medium structures. Depending on the complexity of the medium between the D and A groups, |V| may be predicted using a variety of empirical or theoretical methods.[2] Numerous investigations have delineated the dependence of the D/A electronic coupling on the structure of the medium and have found good agreement between experimental and theoretical results. Still, novel means of effecting and modulating D/A electronic coupling are of considerable interest. Recent studies report that solvent molecules may contribute sizable D/A electronic coupling under specific circumstances.[3−6] In particular, solvent mediated coupling contributions are significant when (1) coupling mediated by covalent connections (the bridge) between a D and an A group is ineffective, (2) solvent molecules readily access the space directly between the D and A groups and make van der Waals contact with both groups, and (3) the electronic properties of the solvent are conducive to electronic coupling.

Nonadiabatic electron-transfer rate constants provide a means to probe the D/A electronic coupling and identify correlations between molecular structure and D/A coupling magnitudes. Extracting this information from rate data requires independent determination of *fcwds* contributions, however. In our prior investigations of solvent mediated coupling, the temperature dependence of the electron-transfer rate data was analyzed to separate *fcwds* and electronic coupling contributions.[3−5] Various models were employed to predict the temperature dependence of the outer sphere reorganization energy λ_o and the reaction free energy $\Delta_r G$. Each model produced a slightly different relationship between the estimated FCWDS, its temperature dependence, and solvent properties. (Note: for clarity, reference to the actual *fcwds* will be indicated by italicized, lower case letters. Calculated FCWDS will be indicated by capitalized, normal type.) Use of molecular solvation models[7] to calculate the FCWDS temperature dependence resulted in solvent independent values of |V| for linear DBA molecules; e.g., compounds **1** and **3** in Scheme 1. By contrast, strongly solvent dependent values of |V| were obtained for highly curved DBA molecules, in which the D and A groups are cofacial and separated by a gap of 7 to 10 Å. Initial characterization of the relationship between coupling magnitude and solvent structure was obtained in this manner.[3,4] Two significant impediments frustrate this approach to delineating structure−coupling correlations. First, the molecular solvation model requires accurate values of numerous solvent properties, both molecular and bulk, to calculate the FCWDS temperature dependence.[7] These parameters are available for a limited number of solvents, thus proscribing the model's general use. Second, the method of analyzing $k_{et}(T)$ data presumes that |V| is temperature independent. This assumption is reasonable in systems where "rigid" covalent bridges propagate the electronic coupling. Its validity is less certain in situations where solvent−substrate interactions mediate the coupling. If |V| varies significantly with temperature,[8] this variation will be incorporated into the *fcwds* analysis and will generate incorrect values for the *fcwds* and |V|.

An alternative procedure for the analysis of electron-transfer rates is employed in this manuscript.[9] Room-temperature electron-transfer data from two linear and one C-shaped molecule are reported in fourteen solvents. The charge-transfer distances in these molecules range from 10 to 12.4 Å. Despite differences in bridge topology, acceptor structure, and driving force among the three molecules, the rate constant data indicate qualitative similarities in the solvent dependence of the electron-transfer rates. The origin of this similarity is investigated using

† Part of the special issue "Noboru Mataga Festschrift".
‡ Chemistry Department, Brown University.
§ Chemistry Department, University of Pittsburgh.

10.1021/jp011603f CCC: $22.00
Published on Web 11/10/2001

SCHEME 1: Line Structures of Molecules 1−4, and CPK Structures of 1−3

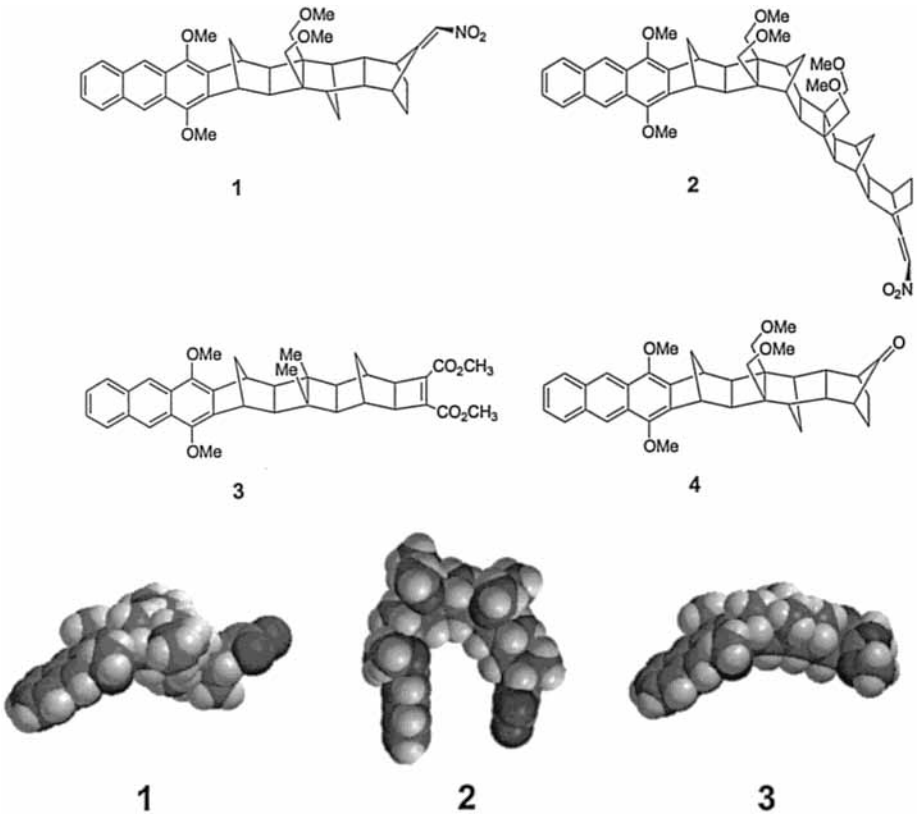

continuum models. This similarity is exploited to probe the dependence of solvent mediated coupling on the solvent molecule's electronic structure.

Experimental Details

Excited-state lifetimes of molecules[10] **1**−**4** (Scheme 1) were determined using picosecond photon counting and nanosecond time-resolved fluorescence methods.[3−5] Sample optical densities at the excitation wavelength (370 or 398 nm) were < 0.15, corresponding to concentrations less than 40 μM. Samples were freeze−thaw-degassed for a minimum of four cycles, and then transferred in vacuo, via a sidearm, to optical quality 1 cm path length cells. The sample temperature was equilibrated to 295 ± 1 K prior to data acquisition. Solvents were dried over Na, CaH or $CaSO_4$ and distilled prior to use. The structures of the solvents and their abbreviations are presented in Scheme 2. The excited-state lifetime τ_4 of the donor only compound **4** was used to determine the intrinsic lifetime of the 1,4-dimethoxyanthracene chromophore in each solvent. Electron-transfer rate constants were determined for each compound, X, using the relationship $k_{et}(X) = 1/\tau_X - 1/\tau_4$. Rate constants are listed in Table 1.

Results and Analysis

Structures of the four molecules investigated are shown in Scheme 1. Each of the molecules contains a 1,4-dimethoxyanthracene chromophore, which serves as the electron donor when in its lowest energy singlet excited state. The electron acceptor in molecules **1** and **2** is a nitroethylene group and is a cyclobutenediester in molecule **3**. Molecule **4** does not have an electron acceptor. It serves as the donor only reference for determination of the electron-transfer rate constants. Space-filling CPK renderings of **1**-**3** are shown at the bottom of Scheme 1. The bridges in molecules **1** and **3** span seven σ-bonds

SCHEME 2: Molecular Structures of the Solvents and Their Abbreviations

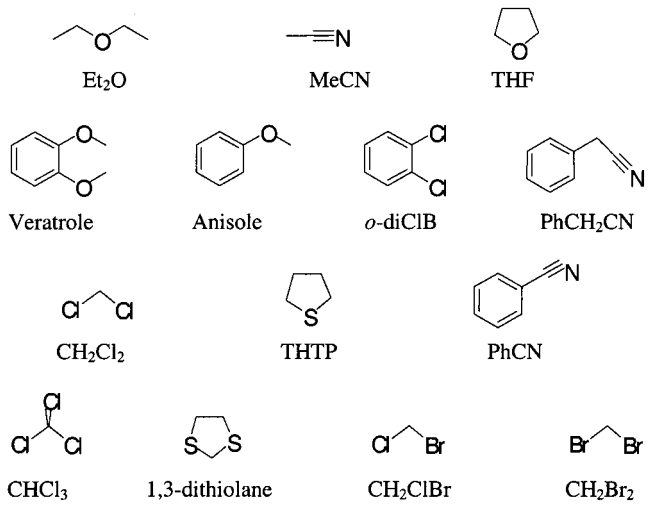

in an all trans configuration and lie in the line of sight between the D and A groups. The charge-transfer distances, R_{CC}, are 12.4 and 11.5 Å, respectively.[11,12] The bridge in molecule **2** spans 11 σ-bonds and incorporates one *s-cis* link. The D and A groups extend from the same face of the bridge, yielding a C-shaped structure. The 10.0 Å gap between the cofacial D and A groups is not obstructed by the bridge and may be occupied by solvent molecules.

Table 1 lists electron-transfer rate constants for molecules **1**−**3** and the excited donor decay rate constant ($k_{S1} = 1/\tau_4$) in fourteen solvents (Scheme 2). The solvents are ordered by ascending rate constant determined for molecule **1**. The electron-transfer rate constants for molecules **2** and **3** exhibit a solvent ordering that is similar to that of **1**, but with some important differences. The transfer rate constants vary by factors of 23,

TABLE 1: Electron Transfer and Donor Only Decay Rate Constants for 1−4 in Fourteen Solvents

solvent	$k_{eT}(1)/10^7\ s^{-1}$	$k_{eT}(2)/10^7\ s^{-1}$	$k_{eT}(3)/10^7\ s^{-1}$	$k_{S1}(4)/10^7\ s^{-1}$
Ethyl Ether	220[a]	1.1[a]	2.0[b]	3.6[a]
Acetonitrile	620[a]	4.7[a]	2.6[b,c]	2.2[a]
Tetrahydrofuran	730[a]	5.4[a]	5.8[b]	3.2[a]
Veratrole	960[d]	10.0[d]	15.2[d]	4.8[d]
Anisole	1160[d]	18.0[d]	13.9[d]	4.1[d]
o-dichlorobenzene	1380[d]	69.3[d]	20.[d]	4.1[d]
$PhCH_2CN$	1560[a]	46.0[a]	15.[d]	3.2[a]
CH_2Cl_2	1600[a]	39.0[a]	6.8[d]	2.5[a]
Tetrahdyrothiophene	1650[d]	20.0[d]	15.8[d]	4.0[d]
PhCN	2400[a]	120.[a]	15.[c]	3.3[a]
$CHCl_3$	2500[a]	100.[a]	26.3[d]	3.9[a]
1,3-dithiolane	2660[d]	62.6[d]	32.[d]	4.7[d]
CH_2ClBr	3500[a]	120.[a]	14.4[d]	5.0[a]
CH_2Br_2	5000[a]	260.[a]	23.4[d]	20.7[a]

[a] Data reported in ref 3c. [b] Data reported in ref 41. [c] Data reported in refs 3a and 5. [d] Data reported here for the first time.

240, and 16 from the slowest solvent (ethyl ether) to the fastest solvent for **1** (CH_2Br_2), **2** (CH_2Br_2), and **3** (1,3-dithiolane), respectively. Within the group of five solvents yielding the slowest rate constants for **1** (ethyl ether, acetonitrile, THF, veratrole, and anisole), the transfer rate constants for **2** and **3** increase, but remain within a factor of 2 of each other. However, in seven of the nine other solvents, the transfer rate constants for the C-shaped DBA molecule, **2**, are from three to eleven times larger than for the linear DBA, **3**. The rate data in Table 1 raise two questions. What factors produce the different ordering of solvents, as gauged by electron-transfer rate constants, for the three DBA molecules? What is the origin of the greater sensitivity to solvent for the transfer rates in molecule **2** as compared to molecules **1** and **3**?

Calibrating the FCWDS. Within semiclassical electron transfer theory,[1] nonadiabatic rate constants k_{et} are calculated as the product of the *fcwds* and the square of the donor−acceptor electronic coupling matrix element, $|V|^2$

$$k_{et} = \frac{2\pi}{\hbar}|V|^2\, fcwds \qquad (1)$$

Experimental rate constant data may be used to examine the solvent dependence of $|V|$, provided the FCWDS can be calculated accurately. Alternatively, rate data can be used to probe the solvent dependence of the *fcwds* if $|V|$ is constant. The bridge in **1** is comprised of an all trans arrangement of σ-bonds and is positioned directly between the D and A groups. In addition, at their points of contact with the bridge, the D and A LUMO's of **1** exhibit the same symmetry with respect to the bridge's mirror plane symmetry element. These factors conspire to make the σ-bonded bridge the only significant source of D/A coupling in **1**, hence $|V(\mathbf{1})|$ should be solvent independent.[13] The variation of electron-transfer rates observed for **1** (Table 1) arises from the solvent dependence of the *fcwds*. The reaction free energy, $\Delta_r G$, and the solvent reorganization energy, λ_o, are the solvent dependent quantities contributing to the *fcwds*. The rate data from **1** can be used to test the accuracy of solvation models' predictions of FCWDS as a function of solvent and to identify whether specific solvation effects are present.

Continuum models provide convenient, albeit simplistic, prescriptions for calculation of $\Delta_r G$ and λ_o from the solvent dielectric constant, ϵ_S, and the refractive index, n_D (see Table 2 for these, and other, solvent properties). These formulas offer insight as to the variations of driving force and λ_o with solvent. When used with the semiclassical rate equation, continuum models often predict trends of rate constant versus solvent that are qualitatively similar to experimental observations.[14] This success stands in sharp contrast to these (continuum) models' erroneous predictions of the temperature dependence of $\Delta_r G$ and λ_o.[15] Simple continuum models account for solvent dipole reorientation but fail to account for density contributions to the solvent response. Density contributions to $\Delta_r G$ and λ_o vary more sharply with temperature than solvent reorientation contributions and must be accounted for when investigating rates as a function of temperature.[16] The objective of this investigation is to understand the solvent dependence of transfer rate constants, preferably without introducing complexities related to any temperature dependence of the *fcwds* or $|V|$. For these reasons, the accuracy of a simple continuum model's prediction of the FCWDS variation with solvent is compared to the observed solvent dependence of the transfer rates for **1** and **3**.

TABLE 2: Solvent Properties

solvent	n_D[a]	ϵ_S[b]	LUMO (eV)	$\lvert V(2)\rvert\ (cm^{-1})$
Ethyl Ether	1.353	4.3	6.46	0.9
Acetonitrile	1.344	37.5	5.77	1.1
Tetrahydrofuran	1.407	7.6	6.21	1.1
Veratrole	1.533	4.4	4.01	1.3
Anisole	1.516	4.3	3.93	1.6
o-dichlorobenzene	1.551	9.9	3.20	2.8
$PhCH_2CN$	1.523	18.7	3.43	2.2
CH_2Cl_2	1.424	8.9	4.19	2.0
Tetrahdyrothiophene	1.504	7.	5.30	1.4
PhCN	1.528	25.2	2.44	2.8
$CHCl_3$	1.446	4.9	3.29	2.5
1,3-dithiolane	1.599	-	4.08	1.9
CH_2ClBr	1.483	8.	3.55	2.4
CH_2Br_2	1.541	7.	3.20	2.9

[a] n_D values obtained from the Aldrich Handbook of Fine Chemicals and Laboratory Equipment, 2000−2001. [b] ϵ_S values obtained from Table 6.3 in ref 38a and from ref 38b.

The continuum expression for the solvent reorganization energy, λ_o, attending electron transfer between two, initially uncharged, spherical donor and acceptor species is given by eq 2

$$\lambda_o = \frac{e^2}{2}\left(\frac{1}{r_A} + \frac{1}{r_D} - \frac{2}{R_{CC}}\right)\left(\frac{1}{{n_D}^2} - \frac{1}{\epsilon_S}\right) \qquad (2)$$

where r_A and r_D are the effective radii of the acceptor and donor groups, R_{CC} is the center to center charge-transfer distance, and $e^2 = 14.4$ eV/Å. The corresponding expression for the free energy change upon electron transfer is given by eq 3

$$\Delta_r G = E_{OX} - E_{RED} - E_{00} - \frac{e^2}{2}\left(\frac{1}{r_A} + \frac{1}{r_D}\right)\left(\frac{1}{\epsilon_{REF}} - \frac{1}{\epsilon_S}\right) - \frac{e^2}{\epsilon_S R_{CC}} \qquad (3)$$

where E_{OX} and E_{RED} are the donor oxidation potential and the acceptor reduction potential, respectively, in a reference solvent (acetonitrile) with static dielectric constant ϵ_{REF}.[17] E_{00} is the $S_1 - S_0$ energy gap in the solvent of interest, with static dielectric constant ϵ_S.[18] Values of 4.5, 3.7, and 3.9 Å were previously established[3c,5] for the effective radii of the anthracene donor, the nitroethylene acceptor and the cyclobutenediester acceptor, respectively, by reproducing λ_o and $\Delta_r G$ values calculated using a finite difference Poisson Boltzman model[19] that takes into account the details of each molecule's shape and the charge distributions of the reduced and oxidized acceptors and donors. Charge-transfer distances, R_{CC}, were calculated using the Generalized Mulliken Hush method.[12] The value of $\Delta_r G$ and λ_o for each DBA structure in each solvent was used to calculate the FCWDS within a single quantized mode, semiclassical model (eq 4)

$$\mathrm{FCWDS} = (4\pi\lambda_o k_B T)^{-1/2} \sum_{n=0}^{\infty} \left(\frac{e^{-S} S^n}{n!} \right) \times \exp[-(\lambda_o + \Delta_r G + nh\nu)^2 / 4\lambda_o k_B T]; \; S = {}^{\lambda_V}/_{h\nu} \qquad (4)$$

A quantized mode energy spacing, $h\nu$, of 0.175 eV was used for each DBA molecule. Previous estimates of the quantized mode reorganization energy (λ_V) were used: 0.30 eV for **1** and **2** and 0.39 eV for **3**.[3c,5] These values are assumed to be solvent independent. Their choice does not influence either the solvent dependence or the relative magnitudes determined for |V| in **1** and **2**.

A plot of the calculated FCWDS versus the experimental electron-transfer rate constants for **1** is displayed in Figure 1A. If the continuum derived FCWDS calculations are correct and |V| is solvent independent, the plotted points should lie on a line with a slope equal to $\hbar/[2\pi|V|^2]$ and an intercept equal to zero. For seven of the eight nonaromatic solvents (solid circles), the calculated FCWDS and the experimental rate constants exhibit a reasonably linear correlation with an intercept that is close to zero. The slope of a linear regression fit to these seven points yields $|V| = 25\ \mathrm{cm}^{-1}$. A previous analysis of the temperature dependence of the rate constant, $k_{et}(T)$, in ethyl ether, acetonitrile and benzonitrile yielded a value of $|V| = 19 \pm 2\ \mathrm{cm}^{-1}$ for the D/A coupling in **1**.[3c] The values of |V| from these independent analyses are in reasonable agreement.

For **1**, the continuum based FCWDS values appear to be consistent with the experimental rate constants in most of the nonaromatic solvents. The points for the six aromatic solvents and THTP are scattered and fall substantially above the regression line for the nonaromatic solvents. In these solvents, the calculated FCWDS are considerably larger than the actual *fcwds*, which are indicated by the position along the experimental transfer rate constant axis. Figure 1B shows an analogous plot for **3**. The linearity of the data in nonaromatic solvents is evident in this system also (with the exception of $CHCl_3$). A linear regression fit of the rate data from the nonaromatic solvents, excluding $CHCl_3$, yields $|V(\mathbf{3})| = 4.9\ \mathrm{cm}^{-1}$. As with **1** the calculated FCWDS values in aromatic solvents are anomalous but not uniformly higher than those for the nonaromatic solvents. Previous investigations[4b,20] have shown that in weakly dipolar solvents, quadrupole moments play a significant role in determining $\Delta_r G$ and λ_o. The simple continuum model used here does not account for solvent quadrupole interactions. Thus, the poor correlation between the continuum derived FCWDS calculations and the experimental rate constants in the aromatic solvents is not surprising. Numerous groups are working to develop solvation theories that incorporate quadrupole contributions.[7a,21] Rate data from **1** and **3** may be of use in benchmarking these theories. For the purposes of this investigation, Figure 1 demonstrates that continuum expressions for $\Delta_r G$ and λ_o generate reasonable estimates of the FCWDS for **1** and **3** in some, but not in all, solvents of interest.

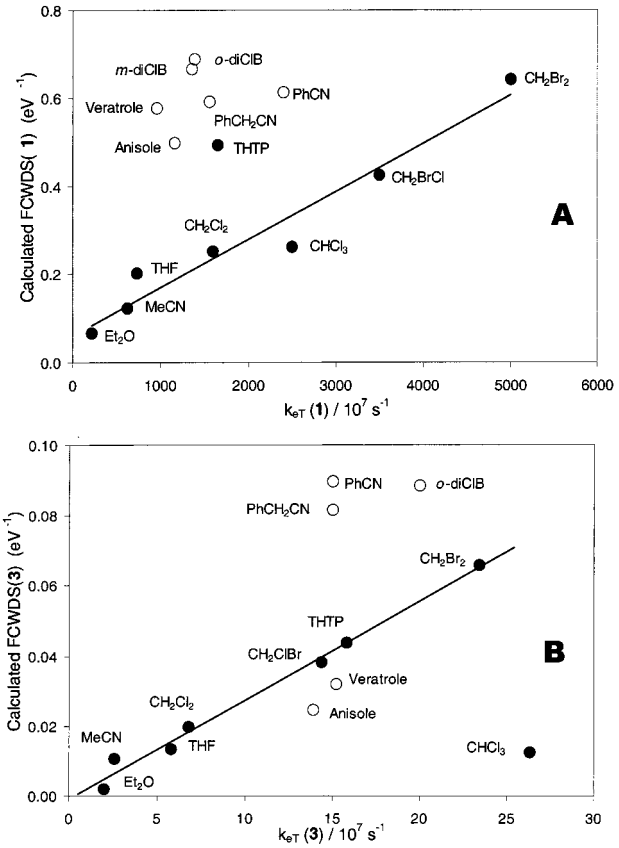

Figure 1. Panel A shows a plot of the Franck Condon Weighted Density of States (FCWDS) calculated for **1** at 295 K using continuum models for $\Delta_r G$ and λ_o vs the experimental transfer rate constants of **1**. Panel B shows a similar plot for **3**. For both panels, the filled circles indicate nonaromatic solvents and the empty circles indicate aromatic solvents. Points for 1,3-dithiolane are not included as ϵ_S of this solvent is unavailable.

The accuracy of FCWDS calculations for **2** is likely to exhibit a similar dependence on solvent type as observed for **1**. As the objective of this study is to determine the solvent dependence of |V| in **2**, an approach is required that generates accurate estimates of the *fcwds* in all solvents. Because **1** and **2** contain identical D and A groups and comparable charge-transfer distances, the solvent dependence of the actual *fcwds* from **1** might be used to predict the solvent dependent *fcwds* for **2**. This approach will be successful if the *fcwds* for **1** and **2** vary proportionally with solvent. Figure 2 (diamonds) displays ratios of the continuum derived FCWDS estimates, FCWDS(**2**)/FCWDS(**1**), versus the observed rate constants for **1**. The experimental rates from **1** are used as the *x*-axis to reflect the change of the actual *fcwds*(**1**) with solvent.[22] For the nonaromatic solvents (filled diamonds), with the exception of ethyl ether, the FCWDS ratio varies from 1.7 to 2.7 with an average value of 2.2 ± 0.4. The predicted FCWDS ratio is slightly smaller for the nonaromatic solvents that provide the fastest rate constants for **1**. Interestingly, the anomalous FCWDS values found for **1** in aromatic solvents (Figure 1) are not manifest when rate ratios are plotted (Figure 2, open diamonds). Continuum models predict relative magnitudes of the FCWDS for **2** and **1** that are reasonably close to the mean value (to within ~30% for all the solvents). Near constancy of the actual *fcwds*

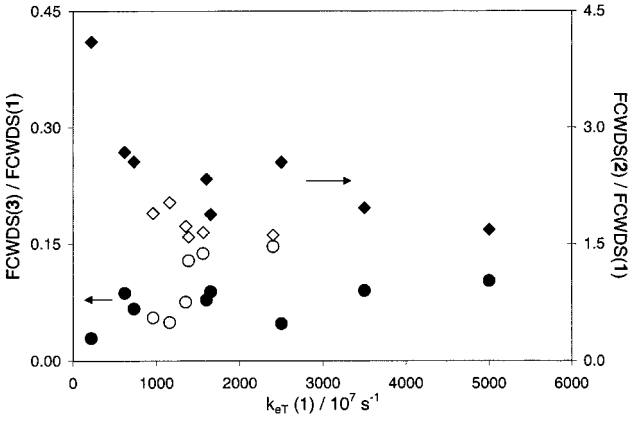

Figure 2. Plots of calculated continuum FCWDS ratios at 295 K for **3**:**1** (circles, left axis) and **2**:**1** (diamonds, right axis) versus the experimental transfer rate constants for **1**. Filled symbols indicate nonaromatic solvents; empty symbols indicate aromatic solvents.

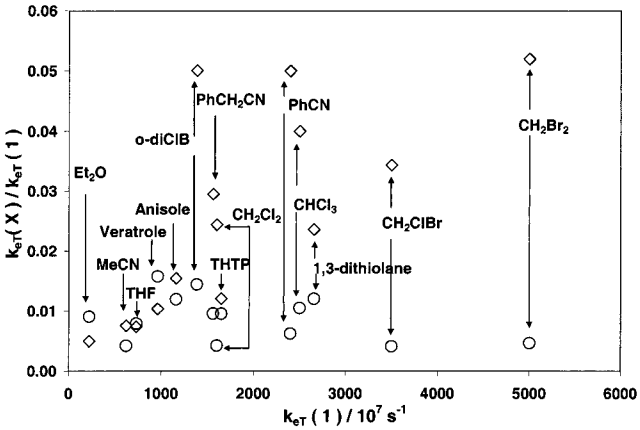

Figure 3. Plots of experimental rate constant ratios $k_{et}(X)$: $k_{et}(\mathbf{1})$ versus the experimental transfer rate constants of **1**. X = **3** (circles) and X = **2** (diamonds). The solvent corresponding to each pair of points is indicated.

ratio for **1** and **2** would provide a simple means to evaluate the solvent dependence of the coupling in **2** (vide infra). However, this prediction cannot be directly verified if |V| for **2** is solvent dependent. For this reason, the accuracy of continuum derived FCWDS ratios will be tested by comparing the solvent dependent FCWDS ratios and rate ratios for **3** and **1**.

As for **1**, the all trans σ-bridge of **3** is the dominant source of D/A coupling and |V(**3**)| should be solvent independent.[3a,5] The charge-transfer distance in **3**, $R_{CC} = 11.5$ Å, is intermediate between that of **1** and **2**. The shape and charge distributions of the reduced acceptors in **1** and **3** are very different. As a result, the variations of $\Delta_r G$ and λ_o with solvent should be dissimilar for **1** and **3**. In addition, the acceptor in **3** affords a substantially smaller driving force for charge separation (by 0.3 eV in MeCN) than does the acceptor in **1**. Given the substantial differences in structure and driving force, comparison of the FCWDS ratios and rate constant ratios for **1** and **3** should constitute a critical test of the continuum model's predictions. Figure 2 shows the continuum derived FCWDS ratio, FCWDS(**3**)/FCWDS(**1**), (circles) plotted versus the solvent dependent transfer rates of **1** (open circles indicate aromatic solvents; filled circles indicate nonaromatic solvents). The predicted ratios are largely independent of solvent, although a slight increase in ratio with increasing transfer rate for **1** may be present. For the nonaromatic solvents, the FCWDS ratios range between 0.029 and 0.10, with an average of 0.074 ± 0.023.[23] This plot indicates that the continuum model predicts comparable scaling of the FCWDS with solvent for **1** and **3** despite the significant differences in the acceptor structures and the driving force for electron transfer in these two DBA molecules. The crucial question is whether the kinetic data for **1** and **3** indicate comparable scaling of the *fcwds* with solvent?

Experimental Rate Ratios (3:1) for Linear Systems. Figure 3 displays the experimental rate constant ratio, $k_{et}(\mathbf{3})/k_{et}(\mathbf{1})$ (circles) plotted versus the rate constants for **1**. The continuum model prediction that FCWDS(**3**)/FCWDS(**1**) does not vary significantly with solvent appears to be supported by the rate constant data. For the nonaromatic solvents, the rate ratio is relatively constant. Upon more critical inspection, the rate ratio decreases slightly with increasing rate of **1**, in contrast to the slight increase predicted by the FCWDS calculations. The scatter in both plots precludes interpreting this difference. The average value of the rate ratio in the nonaromatic solvents is 0.0074 ± 0.0031. For all fourteen solvents, the experimental rate ratio is 0.0089 ± 0.0039. Among solvents with common structural features, the rate ratio exhibits greatly reduced scatter. For example, despite large variations of the transfer rate constants for the three dihalomethane solvents, the rate ratio remains remarkably constant; $< k_{et}(\mathbf{3})/k_{et}(\mathbf{1}) > = 0.0043 \pm 0.003$. In acetonitrile, which also has three heavy (non-hydrogen) atoms, $k_{et}(\mathbf{3})/k_{et}(\mathbf{1})$ equals 0.0042. These values differ substantially from the average value of $k_{et}(\mathbf{3})/k_{et}(\mathbf{1})$ (0.0097 ± 0.0017) in the four, nonaromatic ether and thioether solvents: ethyl ether, THF, tetrahydrothiophene (THTP) and 1,3-dithiolane. The clustering of rate ratios, apparently correlated to the number of heavy atoms in each solvent, may reflect the influence of solvent size on solvation of the different size acceptor groups in **1** and **3** (vide infra). Given that the continuum predictions of the FCWDS (Figure 1, open symbols) are suspect for aromatic solvents, it is encouraging that the experimental rate ratios in the aromatic solvents (Figure 3) are similar to those in the nonaromatic solvents. Still, the five aromatic solvents display the greatest scatter and the largest values of the rate ratio. Values range 2.5-fold, from 0.0060 in benzonitrile to 0.016 in veratrole, with an average $k_{et}(\mathbf{3})/k_{et}(\mathbf{1})$ of 0.012 ± 0.004. Overall, the relatively small variation of the experimental rate ratios for **3** and **1** with solvent is in accord with the continuum derived FCWDS predictions.

The accuracy of D/A electronic coupling magnitudes, derived from rate ratio analyses using calculated FCWDS ratios, may be evaluated using **3,** because |V(**3**)| is solvent independent and can be independently determined using Figure 1B. The D/A coupling for **3** in nonaromatic solvents may be extracted from rate constant ratios using the calculated FCWDS ratios for the nonaromatic solvents and eq 5

$$|V(\mathbf{3})| = |V(\mathbf{1})| \times \sqrt{\frac{k_{et}(3) \times \mathrm{FCWDS}(1)}{k_{et}(1) \times \mathrm{FCWDS}(3)}} \qquad (5)$$

With the reasonable assumption that |V(**1**)| is solvent independent, any *apparent* solvent dependence of |V(**3**)| that this FCWDS ratio approach generates can be assessed.[24] For the three structurally similar, dihalomethane solvents, this analysis yields $|V(\mathbf{3})| = 4.2 \pm 0.2$ cm^{-1}. The value in acetonitrile is comparable; $|V(\mathbf{3})| = 4.2$ cm^{-1}. For the other nonaromatic solvents, this approach yields $|V(\mathbf{3})| = 6.5$ cm^{-1} for THF; 6.2 cm^{-1} for THTP; 8.9 cm^{-1} for chloroform and 10.5 cm^{-1} for ethyl ether. The mean value from this analysis in the nonaromatic solvents is $|V(\mathbf{3})| = 6.1 \pm 2.5$ cm^{-1}. Because the ratio of calculated FCWDS for **3** and **1** is relatively solvent independent (filled circles in Figure 2), the average FCWDS

ratio, 0.074, was also used to evaluate |V(**3**)| in the nonaromatic solvents. The value of |V(**3**)| was found to range from 4.5 to 7.2 cm^{-1}, with an average of 5.7 cm^{-1}.[25] Use of 0.074 as the FCWDS ratio for the aromatic solvents yielded slightly larger |V(**3**)| values, ranging from 5.5 to 8.8 cm^{-1}.[25] Quite clearly, comparable values of |V(**3**)| are obtained by direct analysis of the rate data (Figure 1B) or by analyzing rate ratios. The smallest and largest |V(**3**)| differ by a factor of 2, and the values in aromatic solvents are roughly a third larger than in nonaromatic solvents.[26] Despite large differences in driving force (~0.3 eV) and acceptor structure, the rate constants ratios demonstrate that the actual *fcwds* for **1** and **3** vary comparably with solvent. With the reasonable success of this benchmark, the rate data from **1** and **2** may be analyzed using FCWDS ratios.

Experimental Rate Ratios (2:1) for the C-Shaped Molecule. The presence of identical D and A in **1** and **2** should produce more comparable *fcwds* values and a more similar solvent dependence than found for **1** and **3**. The $k_{et}(\mathbf{2})/k_{et}(\mathbf{1})$ rate ratio data are shown in Figure 3 (diamonds). This graph shows that the solvent dependent electron-transfer rate constants of **2** are poorly predicted by the rate constants of **1**. The rate ratio exhibits large variations for the investigated solvents, even among the four solvents (CH_3CN, CH_2Cl_2, CH_2ClBr, CH_2Br_2) that gave identical values of $k_{et}(\mathbf{3})/k_{et}(\mathbf{1})$. To the extent that an overall trend in the ratios can be identified, it is-to-larger ratios in the solvents supporting the fastest transfer rates for **1**. The poor correlation between the rate constants of **1** and **2** must arise from either very different solvent dependence of the *fcwds* for **2** as compared to **1** and/or a strong solvent dependence of the D/A electronic coupling in **2**. On the basis of the analysis of rate data for **1** and **3** and prior investigations,[3−5] a solvent dependence of |V| is the more likely origin of the scatter in the $k_{et}(\mathbf{2})/k_{et}(\mathbf{1})$ rate plot.

As discussed earlier, the continuum values of the FCWDS ratio for **2** and **1** vary weakly with solvent and have an average ratio of 2.24 in the nonaromatic solvents. Presuming that a single FCWDS ratio is appropriate for all solvents, the D/A coupling for **2** in each solvent may be estimated as $|V(\mathbf{2})| = |V(\mathbf{1})| \times \sqrt{[k_{et}(2)/k_{et}(1)]/2.24}$. Table 2 lists the |V(**2**)| couplings obtained in this way using $|V(\mathbf{1})| = 19$ cm^{-1}. The coupling magnitude varies 3.2-fold: from 0.9 cm^{-1} in ethyl ether to 2.8−2.9 cm^{-1} in benzonitrile, *o*-dichlorobenzene, and methylene bromide. The spread of the |V(**2**)| values is only 1.6 times larger than that observed for **3**. However, the influence of solvent on |V(**2**)| is significantly larger in comparisons made between structurally similar solvents. The predicted FCWDS ratios (**3**:**1** and **2**:**1**), experimental $k_{eT}(\mathbf{3})/k_{eT}(\mathbf{1})$ ratios and |V(**3**)| values are each nearly constant among the three dihalomethane and acetonitrile solvents. By contrast, the $k_{eT}(\mathbf{2})/k_{eT}(\mathbf{1})$ ratios and |V(**2**)| values for these four solvents vary 7-fold and 2.6-fold, respectively. Among aromatic solvents, |V(**3**)| values vary by 60% whereas |V(**2**)| values vary by 210%. Overall, the rate constant and coupling results from **2** provide considerable evidence for solvent dependent coupling.[27]

Origin of the Solvent Dependent Values of |V(2)|. A number of factors influence the magnitude of solvent mediated coupling. Within superexchange models, the number of "pathway" sites (n), the exchange interactions among "pathway" sites (β_{ij}), and the energy gap (Δ) between the tunneling level, and the virtual state, defined by charge transfer to the "pathway" site, determine the coupling.[2,28] If a single solvent molecule comprises the coupling pathway, $n=1$ and the D/A coupling scales as Δ^{-1}; i.e.

$$|V| = \beta_{D^*S}\beta_{SA}/\Delta \quad (6)$$

If the D/A coupling is mediated by vacant orbitals of the solvent (electron mediated superexchange), the relevant superexchange state is D^+S^-A and the corresponding energy gap, Δ, depends on the vertical electron affinity of the solvent. In contrast, if D/A coupling is mediated by filled orbitals of the solvent (hole mediated superexchange), the appropriate superexchange state is $D^*S^+A^-$, and the corresponding energy gap, Δ, depends on the solvent's vertical ionization potential. Previous investigations have found a rough correlation between solvent mediated coupling magnitudes and solvent vertical electron affinities for systems employing excited donors.[3,5] The larger set of solvents in Table 1 allows more extensive investigation of such correlations. Explicit expressions for the energy gap, Δ, between the electron transfer transition state and the mediating superexchange state are likely to be complicated. If the mediating state primarily employs the solvent HOMO, Δ should vary among solvents as $\sim E_{HOMO}$ + constant. If the mediating state involves the solvent LUMO, Δ should vary among solvents as $\sim -E_{LUMO}$ + constant. Either dependence can be probed by plotting $|V|^{-1}$ versus Δ or E_{MO}.[29] Plots of $|V(\mathbf{2})|^{-1}$ versus the solvent HOMO energy are scattered about a best fit regression line that is horizontal. To the extent that the Koopman's theorem applies and the HOMO energy provides a reasonable estimate of the solvent molecule's vertical ionization potential, this result indicates that hole mediated superexchange does not contribute significantly to the electronic coupling. As discussed below, the couplings for **2** display a good correlation with the solvents' LUMO energies. Within the accuracy of Koopman's theorem (i.e., to the extent that the LUMO energy determines the vertical electron affinity), this correlation indicates that the electronic coupling for **2** is dominated by electron mediated superexchange involving solvent molecules.

A plot of |V(**2**)| versus Δ^{-1} should be linear if the exchange coupling terms do not change dramatically with solvent (see eq 6). Although vertical electron affinity provides a good measure of the changes in Δ among different solvents, this quantity is not available for many of the solvents in Table 1. For this reason, the solvent LUMO energy was used instead. Calculations were performed at the Hartree−Fock level using a 6-31G** basis set.[30] The geometry of each solvent molecule was first optimized and then the LUMO energy was determined (see Table 2). Among the solvents for which experimental data is available, the calculated LUMO energies are 2.8 ± 0.3 eV more negative than the literature values of the vertical electron affinity.[31] Figure 4 displays a plot of $|V(\mathbf{2})|^{-1}$ versus solvent LUMO energy. By any reasonable expectation, this plot is linear and provides strong evidence of a correlation between the LUMO energy and the coupling magnitude. This result demonstrates that the D/A mixing for **2** changes significantly as a function on the solvent's electronic structure and that the solvent/solute exchange interactions, β_{ij}, across the 10 Å cleft of **2** are reasonably constant for this group of solvents. The magnitude of $|V(\mathbf{2})|^2$, which is obtained from the experimental rate constants, represents a weighted average over all configurations of solvent molecules within the cleft. The linearity of the correlation in Figure 4 indicates that, in the majority of configurations, a single solvent molecule comprises the superexchange pathway ($n=1$). The slope of a linear regression fit of these data yields an average value of $|\beta_{ij}| = 210$ cm^{-1}.

Discussion

A number of highly curved DBA molecules, employing electronically excited donors, exhibit greatly accelerated electron-

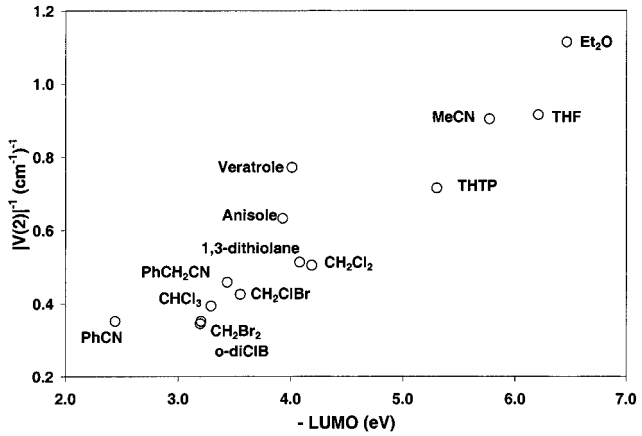

Figure 4. Reciprocal of the D/A coupling magnitude for **2** ($|V(\mathbf{2})|^{-1}$) in each solvent is plotted as a function of the HF 6-31G** LUMO energy of that solvent molecule.

transfer rate constants in electron deficient aromatic and halogenated solvents. The fast rates in these solvents have been attributed to enhanced D*/A coupling involving low energy, unoccupied solvent orbitals. Low lying vacant orbitals support low energy D^+S^-A superexchange states, which enhance mixing between the D* and A sites. This scenario provides a reasonable explanation for the large and rather unusual solvent dependence of electron-transfer rate constants in **2**. However, the solvent dependence of the *fcwds* also contributes to the observed rate variation. This dependence is evident from the behavior of **1** and **3**, which exhibit enhanced electron-transfer rate constants in aromatic and halogenated solvents. Because the linear covalent bridge in **1** and **3** mediates the electronic coupling, |V| in these molecules is expected to be solvent independent. Accordingly, the solvent dependence of the rates for **1** and **3** arises from variation of the *fcwds*. A meaningful analysis of solvent dependent rates and couplings in **2** requires accurate estimates of the *fcwds*.

Characterizing the fcwds. The electron-transfer rates of **1** and **3** in nonaromatic solvents are, for the most part, in accord with the predictions of semiclassical rate constant models using continuum expressions for $\Delta_r G$ and λ_o (Figure 1). Some deviations are evident and may arise from specific solute−solvent interactions. For example, the transfer rate constant for **1** in THTP is about half as large as predicted by the FCWDS calculation. By contrast, the transfer rate constant for **3** in THTP is in good agreement with the FCWDS prediction. The cyclobutenediester group in **3** is a much less potent electron acceptor than nitroethylene. The latter acceptor has been reported to form charge-transfer complexes with good donors.[32] A specific interaction between nitroethylene and THTP, with sulfur acting as a weak donor, would serve to diminish the *fcwds* for D* to A electron transfer and could explain the large upward displacement of the THTP point for **1** from the regression line. Analogous interactions between the sulfurs in 1,3-dithiolane and nitroethylene may explain why this solvent, which has the largest n_D, yields the fastest transfer rate constants for **3**, but not for **1** and **2**.[33] Weak charge-transfer interactions between nitroethylene and anisole or veratrole may be part of the reason that the calculated FCWDS for these two solvents fall well above the regression line for **1** but fall below the regression line for **3**. Automatic inclusion of specific D-solvent or A-solvent interactions is a potential advantage of using the solvent dependent, experimental rate constants from one DBA molecule to gauge the solvent dependent *fcwds* for a second DBA containing the same D and A groups.

The presence of identical D and A groups in two different molecules is not sufficient to ensure comparable *fcwds* solvent dependence. Although identical D and A groups lead to comparable λ_V and $h\nu$ parameters, the driving force and solvent reorganization energy vary with bridge length and topology. The continuum expression for $\Delta_r G + \lambda_o$ and for λ_o (the two solvent dependent terms that appear in the exponent of eq 4.) scale the solvent response by the same geometric factor, $(1/r_A + 1/r_D - 2/R_{CC})$. If the charge-transfer distances, R_{CC}, for two different DBA molecules are such that their geometric factors are very similar, then the two sphere continuum models predict that the solvent dependence of λ_o, of $\Delta_r G + \lambda_o$, and of the FCWDS will be similar for both molecules. The small (14%) difference in the geometric factors for **1**, 0.32, and **2**, 0.28, produces a 2-fold difference in their FCWDS. This difference also generates dissimilar variations of the FCWDS with solvent, most dramatically in solvents with small static, ϵ_S, *and* optical, n_D^2, dielectric constants. This is evident in the FCWDS(**2**)/FCWDS(**1**) ratio for ethyl ether (Figure 2, left most diamond) which is 2-fold larger than for all the other solvents. For the majority of solvents, the FCWDS change comparably for **1** and **2.** Overall, the analysis indicates that the use of the average FCWDS ratio to extract |V| from the rate constant ratios contributes about a ±15% variation in the estimated couplings and represents a relatively small source of error.

The continuum expressions used here for λ_o and $\Delta_r G$ (eqs 1, 2) apply to the case of spherical donor and acceptor ions, with no intervening bridge. The presence of a bridge and the spatial arrangement of the donor, bridge and acceptor groups influence the magnitude of λ_o and $\Delta_r G$, principally through variation of the geometric factor. Barzykin and Tachiya[34] obtained a continuum expression for λ_o in a system composed of contacting donor, bridge, and acceptor spheres. They explored the dependence of the geometric factor on the angle defined by the centers of the three spheres. For angles between 180° and 90°, i.e., from a linear to a right angle DBA geometry, the calculated geometric factor amounted to 94% of the two-sphere value. Between 90° and 60°, the geometric factor decreased to 90% of the two-sphere value. Despite the different DBA topologies of **1** and **2**, the Barzykin-Tachiya result suggests that the appropriate geometric factors for both molecules yield λ_o values that are similar to the two sphere model result and that the topology difference does not produce significant differences in the *fcwds* solvent dependence for the two molecules. The details of the DBA molecule's shape and the D/A ion charge distribution can be included in calculations of λ_o using finite-difference Poisson−Boltzmann (FDPB) methods.[19] The influence of bridge structure on λ_o was previously investigated using two C-shaped and two linear DBA molecules.[5] Assuming the FDPB results to be "correct", the two sphere model was found to significantly underestimate λ_o in C-shaped molecules where R_{CC} is less than or equal to the sum of the D and A spherical radii. The FDPB method's realistic treatment of the donor and acceptor shapes leaves more "continuum solvent" directly between the D and A groups and generates a substantially larger λ_o than the two-sphere expression. For molecules in which R_{CC} is at least a few Å larger than the sum of the D and A radii, the two-sphere model and the FDPB method generated very similar scaling of λ_o with R_{CC}, independent of bridge shape. The FDPB results confirm, at least qualitatively, the conclusions reached by Barzykin and Tachiya.[34] For a given D/A pair, R_{CC} is the dominant term controlling the geometric factor and λ_o; bridge topology provides only a minor perturbation. To the extent that continuum models reproduce the energetics of solvent−solute

interaction, the *fcwds* for the linear and C-shaped DBA molecules **1** and **2** should display similar solvent dependence.

The above arguments imply that the *fcwds* ratios for **3** and **1** should vary little with solvent; however, the experimental rate constant ratio $k_{eT}(\mathbf{3})/k_{eT}(\mathbf{1})$ varies 4-fold in the fourteen solvents. Interestingly, of the five solvents with rate ratios greater than 0.01, veratrole, *o*-dichlorobenzene, anisole, 1,3-dithiolane, and $CHCl_3$, three are likely to experience specific solvent interactions with the nitroethylene acceptor in **1** but not with the acceptor in **3**. Such interactions reduce the transfer rate constant of **1** and generate a larger value of the rate ratio. A fourth solvent, $CHCl_3$, produces an anomalously large rate constant for **3** that may arise from hydrogen bonding interactions involving the acceptor.[35] Ignoring these five solvents, the rate ratio changes by only 2-fold and $|V(\mathbf{3})|$ varies from 4.5 to 6.8 cm^{-1} with an average of 5.6 ± 1.0 cm^{-1}.[36] This value is indistinguishable from the value of 4.9 cm^{-1} derived from a linear fit of the rate constants in Figure 1B. For **3**, D/A coupling is determined equally well from rate or rate ratio analyses. At least a portion of the remaining 2-fold variation of the **3**:**1** rate ratio may arise from the presence of different acceptors in **1** and **3**. More sophisticated continuum and molecular solvation models define an *effective* solute cavity radius that is a function of the solvent size.[7,21,37] The effect of different solvent radii may be mimicked in the simple continuum model by increasing the acceptor radius of **1** and **3** by a constant amount. The hard sphere radii of ethyl ether and THF are ~0.3 Å larger than those of CH_2Cl_2 and MeCN.[38] Increasing the acceptor radius of both **1** and **3** by 0.3 Å increases the calculated FCWDS(**3**)/FCWDS(**1**) ratio by ~30%. This increase is in the same direction, but not as sizable, as the 2-fold larger $k_{eT}(\mathbf{3})/k_{eT}(\mathbf{1})$ ratio found in ethyl ether and THF compared to CH_2Cl_2 and MeCN. Thus, more elaborate continuum models may be required to obtain the most accurate values of $|V|$ when analyzing rate constant ratios from molecules with different D or A groups.

Solvent Dependence of $|V|$. The solvent dependence of the $k_{eT}(\mathbf{2})/k_{eT}(\mathbf{1})$ ratios and the $k_{eT}(\mathbf{3})/k_{eT}(\mathbf{1})$ ratios are dramatically different. Because **1** and **2** possess the same D and A groups, specific solvent effects should cause negligible differences in the *fcwds* of the two molecules. Nor should the different bridge structures cause significant differences in the *fcwds* of **1** and **2**. Rather, the 10-fold variation of the **2**:**1** rate constant ratios arises primarily from solvent dependent electronic coupling in **2**. As the nonadiabatic rate constants are proportional to $|V|^2$, the solvent dependence of the extracted coupling varies less dramatically than the rate constants; by only 3.2-fold for **2** across this set of solvents. Although the following discussion will concern $|V|$, it is important to remember that the kinetically relevant quantity is $|V|^2$.

At least two origins of the solvent dependent electronic coupling in **2** are possible. Solvent may alter the structure of the D, A, or bridge, thus modulating coupling mediated by the bridge. Alternatively, solvent molecules may constitute an independent D/A coupling pathway. Because the same donor and acceptor groups are present in both **1** and **2**, solvent perturbation of D or A structure should appear in both molecules. This might alter the magnitude of bridge-mediated coupling, but the change ought to scale comparably in both molecules and be unobservable in the rate ratio. Solvents might induce changes in bridge structure, e.g., R_{CC} in the clamp might vary with solvent.[39] However, it would be difficult to explain the correlation between coupling magnitude and solvent LUMO energy (Figure 4) in terms of solvent induced changes in bridge structure.[39a] As suggested previously, the more straightforward explanation for the solvent dependent coupling in **2** is the existence of D/A coupling pathways involving a solvent molecule, or molecules, within the cleft. The magnitude of solvent mediated coupling depends on many factors: the energy and spatial distribution of solvent orbitals, solvent size, placement, orientation, and the details of the spatial overlap between the donor and solvent and between the solvent and acceptor. Clearly, the coupling is modulated by solvent motion within, as well as in and out of, the cleft. The coupling magnitudes determined in these analyses are averages over active solvent configurations. The correlation between solvent LUMO energy and coupling magnitude (Figure 4) provides compelling evidence that unoccupied orbitals of the solvent comprise the dominant coupling pathway for DBA **2** in all of the solvents. The average value of $|\beta_{ij}|$, 210 cm^{-1}, is five to 10 times smaller than the exchange interaction determined for aromatic contact ion pairs.[40] Contact ion pairs are more tightly associated than neutral solvent/donor or solvent/acceptor pairs, and the interaction should decrease steeply with increasing separation. These considerations suggest that the derived value of β_{ij} is reasonable for neutral molecules in van der Waals contact.

It is worth noting that use of the average FCWDS ratio to determine $|V(\mathbf{2})|$ (Table 2) reduces the apparent solvent dependence of the coupling. Among the nonaromatic solvents, the trend in Figure 2 (filled diamonds) is to smaller values of the FCWDS ratio in the solvents with the largest $k_{eT}(\mathbf{1})$. Using the predicted FCWDS ratio for each solvent (in an equation analogous to eq 5) reduces the coupling in ethyl ether by 0.2 cm^{-1} ($|V(\mathbf{2})| = 0.7$ cm^{-1}), increases the coupling in CH_2Br_2 by 0.4 cm^{-1} ($|V(\mathbf{2})| = 3.3$ cm^{-1}) and alters the couplings in the other nonaromatic solvents by less than 0.1 cm^{-1}. Thus, $|V|^2$ for **2** in CH_2Br_2 is up to 22 times larger than in ethyl ether and is a primary source of the 240-fold difference of the rate constants in these two solvents.

Conclusion

Solvents strongly influence rate constants of charge separation reactions. In the majority of supramolecular compounds investigated to date, the origin of these rate variations is the solvent dependence of the *fcwds*. For highly curved structures, donor−acceptor electronic coupling can arise from solvent inclusive pathways. In such systems, D/A coupling may be solvent dependent and factoring rate variations into contributions from $|V|^2$ and the *fcwds* is nontrivial. In an effort to identify simple means to effect this separation, photoinduced electron-transfer rate constants were determined for three donor-bridge-acceptor structures in a series of fourteen different solvents. Two of the three structures contained a linear bridge. The rate constants from these linear structures were used (1) to identify and characterize solvent effects on the FCWDS, (2) to evaluate the utility of simple dielectric continuum models of solvation, and (3) to provide a "measure" of the FCWDS solvent dependence for a C-shaped molecule in which D/A coupling is solvent mediated. The solvent dependence of the electron transfer rate constants in the C-shaped molecule was dramatically different from those of the two linear molecules. Using FCWDS estimates derived from the linear structures, the contribution of $|V|^2$ to transfer rates in the C-shaped DBA was found to vary by more than 1 order of magnitude among solvents and to decrease as the energy of the solvent LUMO increases. The correlation with the solvent molecule's LUMO energy demonstrates that unoccupied orbitals of the solvent can be active components of coupling pathways linking excited donor and acceptor groups.

Acknowledgment. We would like to thank Prof. K. Jordan (Pittsburgh) for informative discussions. Financial support from the National Science Foundation is also acknowledged.

References and Notes

(1) Jortner, J. *J. Chem. Phys.* **1976**, *64*, 4860.

(2) (a) Newton, M. D.; *Chem. Rev.* **1991**, *91*, 767. (b) Betts, J. N.; Beratan, D. N.; Onuchic, J. N. *J. Am. Chem. Soc.* **1992**, *114*, 4043. (c) Gray, H. B.; Winkler, J. R. *J. Electroanal.* **1997**, *438*, 43. (d) Paddon-Row: M. N. *Acc. Chem. Res.* **1994**, *27*, 18.

(3) (a) Kumar, K.; Lin, Z.; Waldeck, D. H.; Zimmt, M. B. *J. Am. Chem. Soc*. **1996** ***118,*** 243. (b) Gu, Y.; Kumar, K.; Lin, Z.;.Read, I.; Zimmt, M. B.; Waldeck, D. H. *J. Photochem and Photobiol. A.* **1997**, *105*, 189. (c) Kaplan, R. W.; Napper, A. M.; Waldeck, D. H.; Zimmt, M. B. *J. Am. Chem. Soc.* **2000**, *122*, 12 039.

(4) (a) Read, I.; Napper, A.; Zimmt, M. B.; Waldeck, D. H. *J. Phys. Chem. A*, **2000**, *104*, 9385; b) Read, I.; Napper, A.; Kaplan, R.; Zimmt, M. B.; Waldeck, D. H. *J. Am. Chem. Soc*. **1999**, *121*, 10 976.

(5) Kumar, K.; Kurnikov, I.; Beratan, D.; Waldeck, D. H.; Zimmt, M. B. *J. Phys. Chem. A* **1998**, *102*, 5529.

(6) (a) Loken, N. R.; Paddon-Row: M. N.; Koeberg, M.; Verhoeven, J. W. *J. Am. Chem. Soc.* **2000**, *122*, 5075. (b) Lawson, J. M.; Paddon-Row: M. N.; Schuddeboom, W.; Warman, J.; Clayton, A. H. A.; Ghiggino, K. P. *J. Phys. Chem.* **1993**, *97*, 13 099.

(7) (a) Matyushov, D. V.; Voth, G. A. *J. Chem. Phys.* **1999**, *111*, 3630. (b) Matyushov, D. V. *Chem. Phys.* **1996**, *211*, 46. (c) Matyushov, D. V. *Mol. Phys.* **1993**, *79*, 795.

(8) Evidence for a temperature dependence of solvent mediated coupling in C-shaped DBA molecules has been found. Napper, A.; Read, I.; Zimmt, M. B.; Waldeck, D. H., manuscript in preparation.

(9) A similar analysis of solvent effects on electron transfer rates in highly curved molecules was previously reported. See ref 6a.

(10) Details concerning the preparation of compounds **1** to **4** have been reported elsewhere. (a) Kumar, K.; Tepper, R. J.; Zeng, Y.; Zimmt, M. B. *J. Org. Chem.* **1995**, *60*, 4051. (b) Han, H. Ph.D. Thesis, Brown University, 1998. (c) Kaplan, R. Ph.D. Thesis, Brown University, 2001.

(11) Charge-transfer distances determined using the Generalized Mulliken Hush Methodol. See ref 12.

(12) (a) Cave, R. J.; Newton, M. D. *J. Chem. Phys.* **1997**, *106*, 9213. (b) Cave, R. J.; Newton, M. D. *Chem. Phys. Lett.* **1996**, *249*, 15.

(13) This conclusion is supported by prior determinations of |V| for **1** in three of these solvents; ether, acetonitrile and benzonitrile. See ref 3c.

(14) (a) Chen, P.; Mecklenburg, S. L.; Meyer, T. J. *J. Phys. Chem.* **1993**, *97*, 13126. (b) Heitele, H.; Poellinger, F.; Weeren, S.; Michel-Beyerle, M. E. *Chem. Phys.* **1990**, *143*, 325.

(15) Vath, P.; Zimmt, M. B.; Matyushov, D. V.; Voth, G. A. *J. Phys. Chem. B* **1999**, *103*, 9130.

(16) Molecular solvation models developed by Matyushov incorporate solvent density contributions and reproduce FCWDS variations with temperature accurately. See ref 7, 15.

(17) For the nitroethylene acceptor, $E_{RED} = -1.29$ V. For the cyclobutenediester, $E_{RED} = -1.62$ V. The donor has $E_{OX} = 0.87$ V. All potentials were measured relative to the Ag/AgCl electrode.

(18) E_{00} for the S_1 state of the donor varies between 2.98 and 3.04 eV in these solvents. See Kumar, K. Ph.D. Thesis, Brown University, 1995.

(19) (a) Sharp, K.; Honig, B. *Annu. Rev. Biophys. Biophys. Chem.* **1990**, *19*, 301. (b) Sitkoff, D.; Sharp, K. A.; Honig, B. *J. Phys. Chem.* **1994**, *98*, 8**,** 1978. (c) Zhang, L. Y.; Frieser, R. A. *J. Phys. Chem.* **1995**, *99*, 9, 16 479.

(20) (a) Reynolds, L.; Gardecki, J. A.; Frankland, S. J. V.; Horng, M. L.; Maroncelli, M. *J. Phys. Chem.* **1996**, *100*, 10 337. (b) Khajehpour, Mazdak; Kauffman, John F. *J. Phys. Chem. A* **2000**, *104*, 9512.

(21) (a) Jeon, J.; Kim, H. J. *J. Phys. Chem. A* **2000**, *104*, 9812. (b) Ladanyi, B. M.; Stratt, R. M. *J. Phys. Chem.* **1996**, *100*, 1266. (c) Perng, B.-C.; Newton, M. D.; Raineri, F. O.; Friedman, H. L. *J. Chem. Phys.* **1996**, *104*, 7153, 7177.

(22) As noted above, the coupling across the bridge of **1** is presumed to be solvent independent. Thus, only the FCWDS vary with solvent.

(23) Including all solvents, the calculated FCWDS ratio is 0.085 ± 0.034.

(24) For these calculations, $|V(\mathbf{1})| = 19$ cm^{-1} from a prior evaluation was used. See ref 3c.

(25) The $|V(\mathbf{3})|$ values (in cm^{-1}) obtained using a constant FCWDS ratio are as follows: Et_2O 6.7, MeCN 4.5, THF 6.2, $CHCl_3$ 7.2, CH_2Cl_2 4.6, CH_2ClBr 4.5, THTP 6.8, CH_2Br_2 4.8. For the aromatic solvents, the values are Anisole 7.7, Veratrole 8.8, $PhCH_2CN$ 6.9, PhCN 5.5, o-dichlorobenzene 8.4.

(26) A prior analysis of $k_{eT}(T)$ data for **3** in acetonitrile, dimethylacetamide and benzonitrile yielded $|V(\mathbf{3})| = 2.7 \pm 0.8$ cm^{-1}.[5] This value is 2-fold smaller than the average values derived using the continuum FCWDS. It should be noted that the ratio calculations (FCWDS(**3**)/FCWDS(**1**)) are very sensitive to the values of $\Delta_r G$ in the reference solvent (acetonitrile). The above calculations were based on $\Delta_r G_{ref}(\mathbf{3}) = -0.56$ eV and $\Delta_r G_{ref}(\mathbf{1}) = -0.86$ eV. Lowering the former and raising the latter value by 0.03 eV yields an average value of $|V(\mathbf{3})| = 4.1$ cm-1 for the nonaromatic solvents. Errors in $\Delta_r G_{ref}$ of this magnitude are certainly possible given the presence of electrolyte in the redox measurements.

(27) With the exception of CH_2Br_2, the $|V(\mathbf{2})|$ determined in this analysis are a factor of 2.5 smaller than values derived from analyses of $k_{eT}(T)$ data.[3c] $k_{eT}(T)$ data was analyzed for **2** in MeCN, CH_2Cl_2, $PhCH_2CN$, $CHCl_3$, PhCN, and CH_2Br_2. The values of $|V(\mathbf{2})|$ in CH_2Br_2 was 4.2-fold larger than that obtained in the present analysis. At this point, it is not possible to determine if the larger disparity arises from errors in the parameters used to determine FCWDS(T) or from a stronger temperature dependence of |V| in this solvent.

(28) McConnell, H. M. *J. Chem. Phys*. **1961**, *35*, 508.

(29) Solvent refractive index may also contribute to Δ as the solvent electronic polarizability also solvates the superexchange state.

(30) The calculations were performed using TITAN, Ver. 1.0.5. Wave function and Schroedinger, Inc., 1999.

(31) Discussions of the origin of this offset may be found in the following citations. (a) Chen, D.; Gallup, G. A. *J. Chem. Phys.* **1990**, *93*, 8893. (b) Burrow, P. D.; Howard, A. E.; Johnston, A. R.; Jordan, K. D. *J. Phys. Chem*. **1992**, *96*, 7570. (c) Staley, S. W.; Strnad, J. T. *J. Phys. Chem.* **1994**, *98*, 116.

(32) (a) Kushibiki, N.; Ogasawara, M.; Yoshida, H. *J. Polym. Sci., Polym. Chem. Ed.* **1979**, *17*, 1227. (b) Irie, M.; Tomimoto, S.; Hayashi, K. *J. Polym. Sci., Part B* **1972**, *10*, 699.

(33) The absence of literature dielectric constant data for 1,3-dithiolane prevents calculation of the FCWDS in this solvent.

(34) Barzykin, A. V.; Tachiya, M. *Chem. Phys. Lett*. **1998**, *285*, 150.

(35) Hydrogen bonding strongly accelerates charge separation rate constants of **3** and other linear DBA molecules containing the same D and A. Hydrogen bonding may arise from $HCCl_3$,[35a,b] from ethanol present as stabilizer or from HCl produced when the stabilizer is removed. (a) Phutela, R. C.; Arora, P. S.; Singh, P. P. *Z. Phys. Chem. (Leipzig)* **1976**, *257*, 945. (b) Langner, R.; Zundel, G.; Brzezinski, B. *Spectrochim. Acta, Part A* **1999**, *55A*, 35.

(36) Including *o*-dichlorobenzene, the average value of $|V(\mathbf{3})|$ in the "noninteracting" solvents is 5.9 ± 1.4 cm^{-1}.

(37) (a) Basilvesky, M. V.; Rostov, I. V.; Newton, M. D. *Chem. Phys.* **1998,** *232*, 189. (b) Newton, M. D.; Basilevsky, M. V.; Rostov, I. V. *Chem. Phys.* **1998**, *232*, 201.

(38) (a) Marcus, Y. *Ion Solvation*, John-Wiley and Sons: Chichester, 1985. Table 6.4. (b) Schmid, R.; Matyushov, D. V. *J. Phys. Chem*. **1995**, *99*, 2393.

(39) (a) Calculations by Paddon-Row and co-workers[39b] suggest that pyramidalization of reduced ethylene acceptors reduces the charge-transfer separation, R_{CC}, after electron transfer in C-shaped molecules in a vacuum. The reduction of R_{CC} in **2** could vary with solvent polarity and influence its electron-transfer kinetics. The extent of this Coulomb driven reduction of the D/A separation, if it occurs in solution, should be largest in solvents with the smallest dielectric constants. The observed variation of $|V(\mathbf{2})|$ is not correlated with dielectric constant. (b) Shephard, M. J.; Paddon-Row: M. N. *J. Phys. Chem. A* **2000**, *104*, 11 628.

(40) Gould, I. R.; Young, R. H.; Mueller, L. J.; Albrecht, A. C.; Farid, S. *J. Am. Chem. Soc.* **1994**, *116*, 3147.

(41) Zeng, Z.; Zimmt, M. B. *J. Am. Chem. Soc.* **1991**, *113*, 5107.